Data Pattern Dependence of the Total Ionizing Dose Effect in 3D NAND Flash Memories

Taiki Ozawa†, Kazutoshi Kobayashi†, and Jun Furuta ‡
† Dept. of Electronics, Kyoto Institute of Technology, Japan
‡ Dept. of Info. and Comm. Eng., Okayama Prefectural University, Japan

***Abstract*—The total ionizing dose effect (TID) is one of radiation effects that must semiconductor chips for outer space use. We have evaluated the TID characteristics for each data pattern in triple level cell (TLC) floating-gate and charge-trap NAND flash memories. Gamma-ray irradiation measurements showed that the TID characteristics of the charge-trap type depend more on the data pattern than those of the floating-gate type. The charge-trap type has high TID tolerance for data patterns with small cell threshold voltages shifts, but the tolerance significantly decreases as the threshold voltage increases.**

***Index Terms*—3D NAND flash, floating gate, charge trap, Total Ionizing Dose Effect (TID), Triple Level Cell(TLC)**

I. Introduction

NAND flash memory is a large-capacity, low-power, compact, lightweight nonvolatile memory. It is attracting attention as a memory device for spacecrafts. However, unlike hard drives, flash memory is affected by the TID, which is one of radiation effects. TID is a phenomenon in which device characteristics are changed by the electric charge generated by the ionizing effect of charged particle [1].

Flash memory can be classified into floating gate (FG) type and charge trap (CT) type. The FG type stores electrons in a conductor to retain values. The CT type retains electrons in defects in the CT layer, which is an insulating layer [2]. In flash memory, TID decreases the threshold voltage (V_{th}), resulting in a change in retained value [3]. In general, the CT type has been shown to be more TID resistant than the FG type [4]. Triple Level Cell (TLC), which stores three bits in a single cell, is suitable for space probes designed for long-distance flights and for storage elements in satellites that handle large amounts of data. However, compared to single-level cells, multi-level memory is prone to changes in retained values due to TID because of the small read margin of the V_{th}. Because the V_{th} of a cell differs depending on stored data patterns, it is necessary to evaluate the radiation characteristics of each data pattern. However, a detailed investigation of TID resistance for each TLC data pattern has not yet been conducted.

In this paper, we compare the TID characteristics of FG type and CT type TLC flash memories for each data pattern. The distribution of the respective threshold voltages was measured immediately after gamma-ray irradiation, and the data pattern dependence of the TID characteristics was evaluated and analyzed.

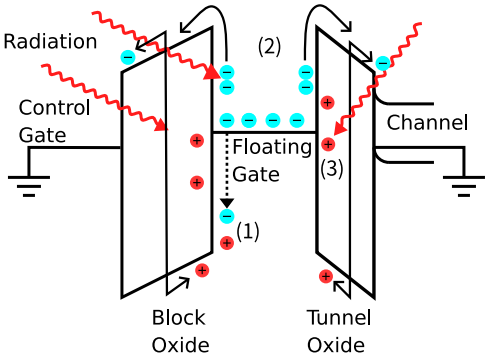

Fig. 1: V_{th} reduction by TID

II. TID in flash memories

TID in flash memory decreases V_{th} and degrades of data retention characteristics. Fig. 1 shows the three main mechanisms of TID generation in the FG type.

1) Radiation to the oxide film generates electron-hole pairs. Some of the holes are sent to the floating gate (FG) due to the electric field in the oxide film and recombine with electrons. The amount of stored electrons in the cell decreases and V_{th} decreases, resulting in a change in the stored value. This effect occurs only in flash memory, which has a structure that stores electrons inside the gate. Since the amount of holes delivered to the FG depends on the electric field applied to the oxide film, the higher the cell V_{th}, the greater this effect [5].
2) The energy of the radiation causes electrons held in the FG to be released beyond the height of the oxide film barrier to the control gate or substrate. As a result, V_{th} decreases [5].
3) Some of the holes generated by irradiation to the oxide film are trapped in interface levels and defects, causing V_{th} to shift. However, this effect is small compared to 1) and 2) because the oxide film becomes thinner as process scaling [6] [7].

III. Flash memories

Fig. 2 shows FG and CT type 3D flash memories. The planar structure is facing the limit of miniaturization due to interference between cells and a decrease in the number of stored electrons. Different from the 2D structure, the 3D

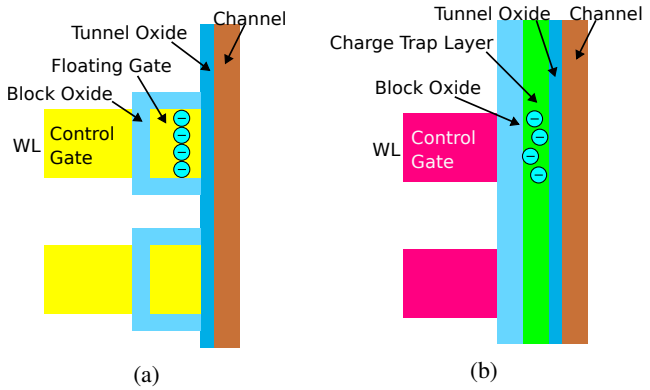

Fig. 2: Cross sections of 3D FG (a) and CT (b) type flash memories

structure has stacked word lines to increase the bit density [8].

Flash memories are classified into FG and CT depending on the structure that holds electrons. The FG type stores data by storing electrons in the FG between oxide films. The FG is usually made of polysilicon, and the stored charge is free to move within the FG. In contrast, the CT type stores charge in defects in the charge trap layer. Since the CT layer is made of silicon nitride, which is an insulator, the trapped electrons cannot move within the CT layer. In general, the CT type has been shown to have stronger radiation resistance [9]. This is because the electrons are discretely trapped and less likely to recombine with holes migrating from the oxide film, allowing the holes to escape to the substrate and control gate. On the other hand, in the FG type, electrons are free to move. Recombination with transferred holes invariably occurs, and V_{th} is greatly reduced [4].

In NAND flash memories, the amount of charge stored in the gate of each memory cell determines the stored value. The number of bits that can be stored in a cell defines the cell type. Different products of multi-level memories have different data patterns assigned to each V_{th}. Generally, adjacent memory values have a Hamming distance of one to facilitate error correction. As the number of retained bits per cell increases, reliability deteriorates because the margin of V_{th} between adjacent levels becomes smaller [10]. Depending on the data pattern, the amount of charge in the gate and the electric field applied to the oxide film are different. Therefore, in multi-level memory, radiation characteristics change depending on the data pattern.

IV. MEASUREMENT SETUPS

Two types of flash memory chips detached from commercial SSDs were used as measurement targets. Table I shows the specifications of the chips. The distribution of data patterns to V_{th} differs between the FG and CT types, as shown in the Fig. 3. Fig. 4 shows the measurement setups. Erasing, programming, and reading were performed using SIGLEAD

TABLE I: Specifications of FG and CT type flash memory chips

Type	Floating gate (FG)	Charge trap (CT)
Model	Intel 29F01T2ANCTH2	KIOXIA TABHG65AWV
Structure	64 layer TLC 3D NAND	96 layer TLC 3D NAND
Package	BGA 132	
Capacity	256 Gb	512 Gb
Block size	9 MB	16 MB
Page size	4 KB	16KB

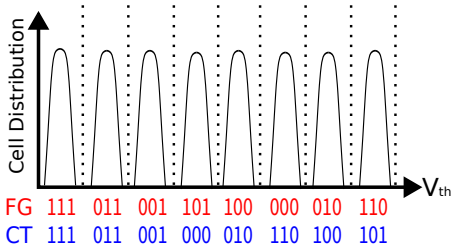

Fig. 3: Distribution of data patterns with respect to V_{th} for FG and CT types

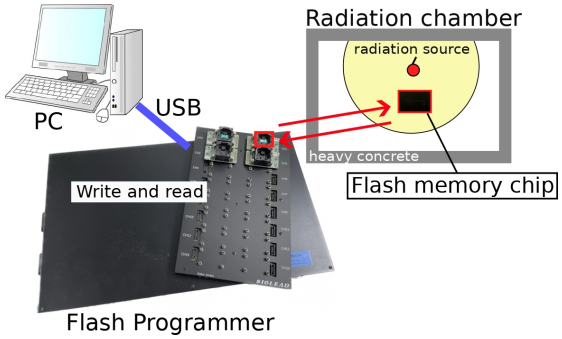

Fig. 4: Measurement setups. PC, SigNAS3, Irradiation room

inc's SigNAS3, a dedicated flash memory tester, connected to the host PC with a USB cable. Gamma-ray irradiation tests were conducted using the Co-60 radiation source at the National Institutes for Quantum Science and Technology. Only memory chips were placed in the irradiation chamber, and write and read operations were done outside the irradiation room.

The procedure is shown below. First, random values were wtitten to one block of each FG type and CT type chip before irradiation. Then they were irradiated and the distribution of V_{th} and bit error rate (BER) were measured. The chips were placed in the irradiation chamber and irradiated with 25 krad(Si) gamma-rays in 30 minutes. Immediately after irradiation, the V_{th} distribution and BER of the measurement block were measured. Since this experiment was an accelerated test and irradiation was performed at a high dose rate for a short time, many holes released from the interface level immediately after irradiation. Because it is necessary to take into account the effect of holes released over time, the irradiated chips were left at room temperature. After that, the distribution of V_{th} and

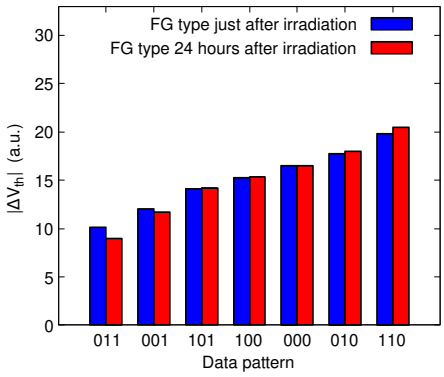

(a)

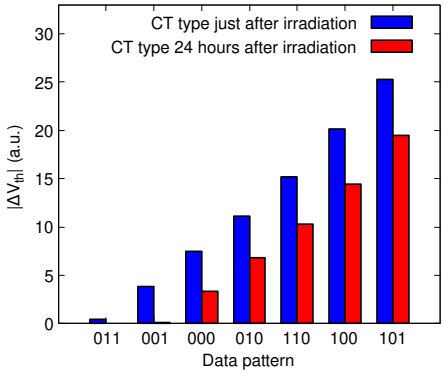

(b)

Fig. 5: Shifts in V_{th} after irradiation and after 24 hours at room temperature. FG type is shown in (a) and CT type in (b).

BER were measured again.

V. MEASUREMENT RESULTS

The V_{th} shift from before irradiation is defined as ΔV_{th}. It is calculated from the difference of the average values of the distribution. Fig. 5 shows $|\Delta V_{th}|$ due to gamma-ray irradiation and $|\Delta V_{th}|$ after leaving the device at room temperature for 24 hours. The V_{th} and $|\Delta V_{th}|$ are expressed in arbitrary units (a.u.). The higher V_{th} of a data pattern, the larger the decrease in V_{th} due to gamma-ray irradiation. In the FG type, the data pattern dependence of the shift was small. In the CT type, the decrease in V_{th} of the data pattern with low V_{th} was extremely small. However, Fig. 5 shows $|\Delta V_{th}|$ increased significantly as V_{th} of the data pattern increases. In the CT type, $|\Delta V_{th}|$ decreased at 24 hours after irradiation compared to that immediately after irradiation. A portion of the reduced V_{th} was recovered by leaving at room temperature. On the other hand, $|\Delta V_{th}|$ was almost unchanged for the FG type before and after leaving at room temperature. Fig. 6 shows the measured distribution of V_{th} for each data pattern. The higher Vth of the data patterns decreased the Vth, and the variance increased by up to 35 % with 25 krad gamma-ray radiation.

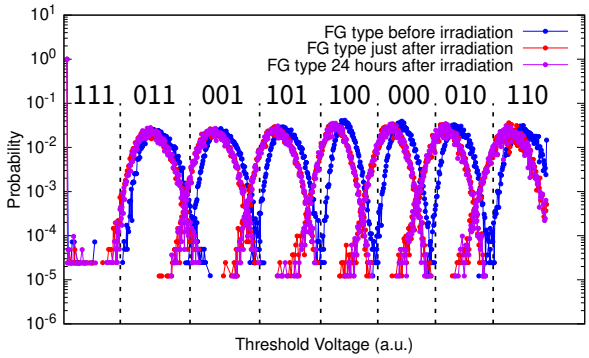

(a)

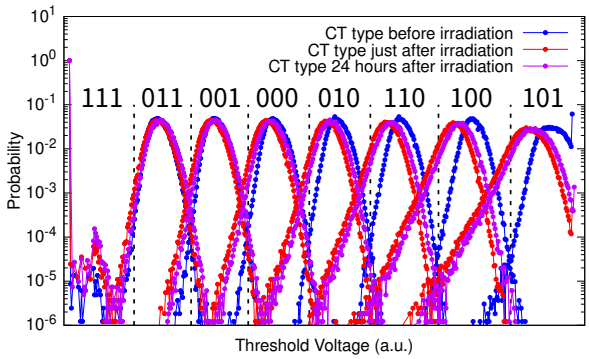

(b)

Fig. 6: Probability distribution of V_{th} for each data pattern of FG (a) and CT (b). Each horizontal axis has a different voltage per unit.

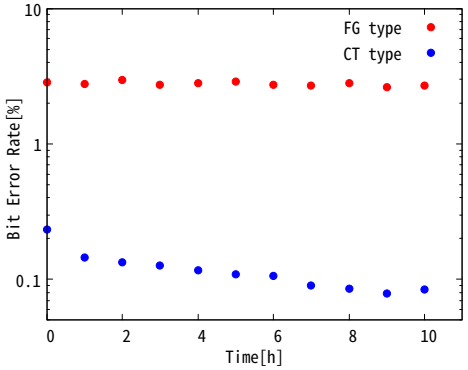

Fig. 7: BER according to time after irradiation

Fig. 7 shows the BER as a function of time after irradiation. The BER in the unirradiated state was 0.019 % for the FG type and 0.0059 % for the CT type. In the FG type, the BER after irradiation increased significantly to 2.9 %. The BER of the FG type remained constant during room leaving it at temperature and no recovery was observed. The BER of the CT type was 0.26 % immediately after irradiation and decreased to 0.095 % after 10 hours of exposure at room temperature.

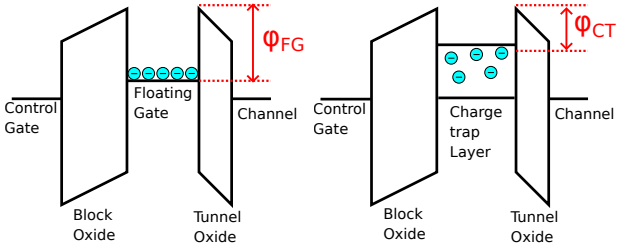

(a) FG type (b) CT type

Fig. 8: Work function (φ) in flash memory

VI. DISCUSSION

The reason that CT type data patterns with low V_{th} have high TID resistance is that recombination is less likely to occur in the CT layer. Electrons trapped in the CT film cannot move freely. Therefore, recombination with holes migrating from the oxide film is hard to occur. Because holes that do not recombine are ejected to the control gate or substrate, they do not contribute to a decrease in the cell V_{th}. On the other hand, in the FG type, electrons are captured in the conductor and can move freely. Even for data patterns with a small number of electrons, such as 011, recombination with the moving holes occurs at a high probability, resulting in a decrease in the cell's V_{th}. $|\Delta V_{th}|$ increases slightly for data patterns with larger V_{th} because of the larger electric field in the oxide film. The high data pattern dependence of the CT type is due to the large amount of electrons discharged by gamma-ray irradiation. The CT type stores electrons by trapping them in defects in the CT layer. As shown in the Fig. 8, the CT type has a small work function (φ), so it tends to discharge a large number of electrons due to gamma-ray ray irradiation. This effect is larger for data patterns with higher V_{th}, which trap more electrons.

The reason why V_{th} recovers is because holes that have been trapped without recombining escape to the control gate and substrate over time. The CT type has a larger recovery because the holes sent to the CT film are less likely to recombine with electrons, and a higher percentage of them are trapped by defects. These holes are discharged over time, and the V_{th} is recovered. Therefore, the BER increased by gamma-ray irradiation decreases with time after irradiation. In the FG type, the recovery is small because most of the holes are used for recombination. BER increases temporarily due to gamma-ray irradiation, but BER decreases over time.

This experiment is an acceleration test, and gamma-ray rays are irradiated at a higher dose rate and for a shorter time than in space. In space, where low dose rate and long irradiation times are expected, recovery effects occur during irradiation. The better the recovery characteristics, the less degradation in space. Based on the above, the CT type is more resistant to radiation in space than the FG type.

VII. CONCLUSION

We used gamma-ray radiation to investigate the radiation tolerance of TLC flash memory and evaluated the data pattern dependence of TID characteristics from the threshold distribution and BER of two types of flash memory. The FG type TLC flash memory exhibits low data pattern dependence and low TID tolerance for any data pattern. The CT type has higher TID tolerance than the FG type, but shows strong data pattern dependence. The CT type demonstrates excellent TID tolerance for data patterns with low V_{th}, but the tolerance is weaker for data patterns with high V_{th}. This is due to differences in the structure that holds electrons, which must be considered when flash memory is used in space. The radiation tolerance of the CT type TLC can be improve by increasing the readout margin of data patterns with high V_{th}. Only the CT type shows recovery when left at room temperature. This is expected to suppress degradation due to TID in space, where flash memory is exposed to low dose rate radiation for long periods of time. Compared to the measured results, the CT type is considered to show much higher radiation resistance in space than the FG type.

ACKNOWLEDGMENT

The authors would like to thank to QST (National Institutes for Quantum and Radiological Science and Technology) for gamma ray experiments.

REFERENCES

[1] Z. Yuan, M. Qiao, X. Li, D. Hou, S. Zhang, X. Zhou, Z. Li, and B. Zhang, "Improved model on buried-oxide damage induced by total-ionizing-dose effect for hv soi ldmos," *IEEE Transactions on Electron Devices*, vol. 68, no. 4, pp. 2064–2070, 2021.

[2] M. Raquibuzzaman, M. M. Hasan, A. Milenkovic, and B. Ray, "Layer-to-layer endurance variation of 3d nand flash memory," in *2022 IEEE International Reliability Physics Symposium (IRPS)*, 2022, pp. 1–5.

[3] G. Cellere, P. Pellati, A. Chimenton, J. Wyss, A. Modelli, L. Larcher, and A. Paccagnella, "Radiation effects on floating-gate memory cells," *IEEE Transactions on Nuclear Science*, vol. 48, no. 6, pp. 2222–2228, 2001.

[4] J. Bi, "Radiation effects of floating-gate (fg) and charge-trapping (ct) flash memory technologies," in *2019 International Conference on IC Design and Technology (ICICDT)*, 2019, pp. 1–3.

[5] M. J. Marinella, "Radiation effects in advanced and emerging nonvolatile memories," *IEEE Transactions on Nuclear Science*, vol. 68, no. 5, pp. 546–572, 2021.

[6] M. Buddhanoy, P. Kumari, U. Surendranathan, M. Wasiolek, K. Hattar, and B. Ray, "Total ionizing dose effects on long-term data retention characteristics of commercial 3-d nand memories," *IEEE Transactions on Nuclear Science*, vol. 69, no. 3, pp. 390–396, 2022.

[7] M. Bagatin, S. Gerardin, G. Cellere, A. Paccagnella, A. Visconti, M. Bonanomi, and S. Beltrami, "Error instability in floating gate flash memories exposed to tid," *IEEE Transactions on Nuclear Science*, vol. 56, no. 6, pp. 3267–3273, 2009.

[8] P. Kumari, S. Huang, M. Wasiolek, K. Hattar, and B. Ray, "Layer-dependent bit error variation in 3-d nand flash under ionizing radiation," *IEEE Transactions on Nuclear Science*, vol. 67, no. 9, pp. 2021–2027, 2020.

[9] H. Hu, Y. Feng, X. Zhan, K. Xi, L. Ji, J. Chen, and J. Liu, "Experimental characterizations on tid radiation impacts in charge-trap 3d nand flash memory," in *2021 Silicon Nanoelectronics Workshop (SNW)*, 2021, pp. 1–2.

[10] N. Papandreou, H. Pozidis, N. Ioannou, T. Parnell, R. Pletka, M. Stanisavljevic, R. Stoica, S. Tomic, P. Breen, G. Tressler, A. Fry, T. Fisher, and A. Walls, "Open block characterization and read voltage calibration of 3d qlc nand flash," in *2020 IEEE International Reliability Physics Symposium (IRPS)*, 2020, pp. 1–6.